

Optical determination of the superconducting energy gap in electron-doped $\text{Pr}_{1.85}\text{Ce}_{0.15}\text{CuO}_4$

C. C. Homes,^{1,*} R. P. S. M. Lobo,² P. Fournier,³ A. Zimmers,⁴ and R. L. Greene⁴

¹*Condensed Matter Physics & Materials Science Department,
Brookhaven National Laboratory, Upton, New York 11973, USA*

²*Laboratoire de Physique du Solide (UPR 5 CNRS) ESPCI, 10 Rue Vauquelin 75231 Paris, France*

³*Département de Physique, Université de Sherbrooke, Sherbrooke, Québec, J1K 2R1 Canada.*

⁴*Center for Superconductivity Research, Department of Physics,
University of Maryland, College Park, MD 20742, USA*

(Dated: February 6, 2008)

The optical properties of single crystal $\text{Pr}_{1.85}\text{Ce}_{0.15}\text{CuO}_4$ have been measured over a wide frequency range above and below the critical temperature ($T_c \simeq 20$ K). In the normal state the coherent part of the conductivity is described by the Drude model, from which the scattering rate just above T_c is determined to be $1/\tau \simeq 80 \text{ cm}^{-1}$. The condition that $\hbar/\tau \approx 2k_B T$ near T_c appears to be a general result in many of the cuprate superconductors. Below T_c the formation of a superconducting energy gap is clearly visible in the reflectance, from which the gap maximum is estimated to be $\Delta_0 \simeq 35 \text{ cm}^{-1}$ (4.3 meV). The ability to observe the superconducting energy gap in the optical properties favors the nonmonotonic over the monotonic description of the d -wave gap. The penetration depth for $T \ll T_c$ is $\lambda \simeq 2000 \text{ Å}$, which when taken with the estimated value for the dc conductivity just above T_c of $\sigma_{dc} \simeq 35 \times 10^3 \text{ } \Omega^{-1}\text{cm}^{-1}$ places this material on the general scaling line for the cuprates defined by $1/\lambda^2 \propto \sigma_{dc}(T \simeq T_c) \cdot T_c$. These results are consistent with the observation that $1/\tau \approx 2\Delta_0$, which implies that the material is not in the clean limit.

PACS numbers: 74.25.Gz, 74.25.-q, 74.72.-h

I. INTRODUCTION

The high-temperature copper-oxide superconductors may be grouped into two broad categories; hole- and electron-doped materials. The hole-doped materials constitute the majority of the cuprate superconductors, while electron doping is observed in a relatively small number of materials, mainly the $(\text{Nd,Pr})_{2-x}\text{Ce}_x\text{CuO}_4$ systems^{1,2} and the infinite-layer $(\text{Sr,L})\text{CuO}_2$ ($L = \text{La, Sm, Nd, Gd}$) materials.^{3,4} The phase diagrams of the hole- and electron-doped materials have some similarities,⁵ with the parent materials being antiferromagnetic (AFM) insulators in both cases. However, the electron-doped materials are also noticeably different in that the AFM region extends to a much higher doping with an almost non-existent pseudogap region.^{6,7,8} In addition, the superconducting dome is quite small, with relatively low critical temperatures (T_c 's). These differences have prompted some debate as to whether or not the electron-doped materials were high-temperature superconductors at all, or if they resembled more conventional superconductors. While some work indicated that the electron-doped materials possess an isotropic s -wave superconducting energy gap,^{9,10} more recent studies have suggested that the energy gap has nodes and is d -wave in nature,^{11,12,13,14,15,16,17,18,19,20,21} similar to the hole-doped materials.^{22,23} However, while the d -wave gap in the hole-doped materials may be described in a monotonic way, $\Delta(\phi) = \Delta_0 \cos(2\phi)$, where Δ_0 is the gap maximum and ϕ is a Fermi surface angle, the energy gap in the electron-doped materials appears to be nonmonotonic, i.e., $\Delta(\phi) = \Delta_0 [\cos(2\phi) - a \cos(6\phi) + b \cos(10\phi)]$.^{18,19,20}

In electron-doped materials, a pseudogap exists in the underdoped regime and overlaps superconductivity over a small portion of the phase diagram.^{24,25} In the normal state above the superconducting dome, the conductivity is reasonably metallic.²⁴ The formation of a superconducting energy gap and the commensurate change in the density of states (DOS) should lead to observable changes in the low-energy optical properties. In initial optical studies of the electron-doped $(\text{Nd,Pr})_{2-x}\text{Ce}_x\text{CuO}_4$ materials,^{24,26,27,28,29,30,31,32,33,34} there was no definitive signature in the reflectance of a gap opening. It was suggested that this was due to the fact that the high-temperature superconductors were in the clean limit (i.e., the regime where the normal-state scattering rate $1/\tau \ll \Delta_0$, or alternatively when the mean free path is much greater than the coherence length, $l \gg \xi_0$), where the formation of a superconducting gap is difficult to observe.³⁵ Interestingly, we have recently observed changes in the reflectance of thin films of $\text{Pr}_{2-x}\text{Ce}_x\text{CuO}_4$ above and below T_c which track with doping,³⁶ indicating that these features are associated with the superconducting energy gap. However, in any study of thin films there is always the concern that substrate-induced strain may affect the structural and electronic properties of the film.

In this work we examine the optical properties of an optimally-doped single crystal of $\text{Pr}_{1.85}\text{Ce}_{0.15}\text{CuO}_4$ ($T_c \simeq 20$ K) for light polarized in the copper-oxygen planes over a wide frequency range in the normal and superconducting states. Some aspects of this work have been previously reported.³⁷ The results show a clear signature of the formation of a superconducting energy gap in the reflectance and the optical conductivity, validat-

ing the earlier thin-film work.³⁶ The normal-state properties are well described by a simple two-component model (coherent and incoherent components), which allows the plasma frequency of the coherent Drude component ω_{pd} and the scattering rate $1/\tau$ to be determined. At 30 K, $1/\tau \simeq 80 \text{ cm}^{-1}$ or about 10 meV, which is consistent with the observation that $\hbar/\tau \approx 2k_B T$ near T_c in many of the cuprate superconductors. In the superconducting state, the real part of the dielectric function and optical conductivity sum rules both yield estimates for the in-plane penetration depth of $\lambda \simeq 2000 \text{ \AA}$. From the structure observed in the reflectance below T_c , the gap maximum is estimated to be $\Delta_0 \simeq 35 \text{ cm}^{-1}$ (about 4.3 meV). For values of $1/\tau$ determined just above T_c , the result that $1/\tau \approx 2\Delta_0$ (valid primarily along the antinodal direction) indicates that the material is not in the clean limit, in agreement with recent scaling arguments.^{38,39} In addition, we speculate that the nonmonotonic nature of the superconducting gap in this material results in large changes to the joint density-of-states (JDOS) below T_c relative to the monotonic case, allowing the formation of the gap to be observed more easily in the optical response.

II. EXPERIMENTAL

Single crystals of $\text{Pr}_{1.85}\text{Ce}_{0.15}\text{CuO}_4$ were grown from a CuO-based flux using a directional solidification technique.⁴⁰ A mixture of high-purity (99.9%) starting materials of Pr_6O_{11} , CeO_2 and CuO were heated rapidly to just above the melting point ($\sim 1270^\circ\text{C}$ for this Ce concentration). After a soak of several hours at the maximum temperature, the materials were cooled slowly to room temperature. To induce superconductivity, the crystals (typical size of $2 \times 2 \text{ mm}^2$ and $\sim 20 \mu\text{m}$ thickness) were oxygen reduced by annealing in an inert gas atmosphere following a procedure similar to that described by Brinkmann *et al.*⁴¹ The superconducting transition was characterized by a SQUID magnetometer from Quantum Design in a field of 1 Oe (ZFC), and the critical temperature determined to be $T_c \simeq 20 \text{ K}$. The observed value of T_c for this Ce concentration is somewhat less than ideal, suggesting that the sample may have been over-reduced.

The reflectance of single-crystal $\text{Pr}_{1.85}\text{Ce}_{0.15}\text{CuO}_4$ has been measured at a near-normal angle of incidence for light polarized in the a - b planes from ≈ 18 to over 34000 cm^{-1} , above and below T_c , on Bruker IFS 66v/S and IFS 113v spectrometers using an *in-situ* evaporation technique.⁴² The noise in the far-infrared reflectance is less than 0.05%, resulting in a signal-to-noise ratio of better than 2000 : 1. The optical properties are calculated from a Kramers-Kronig analysis of the reflectance, where extrapolations are supplied for $\omega \rightarrow 0, \infty$. At low frequency, a metallic Hagen-Rubens response is assumed in the normal state ($R \propto 1 - \omega^{1/2}$), and a two-fluid model was applied in the superconducting state ($R \propto 1 - \omega^2$). Above the highest-measured frequency in this experiment

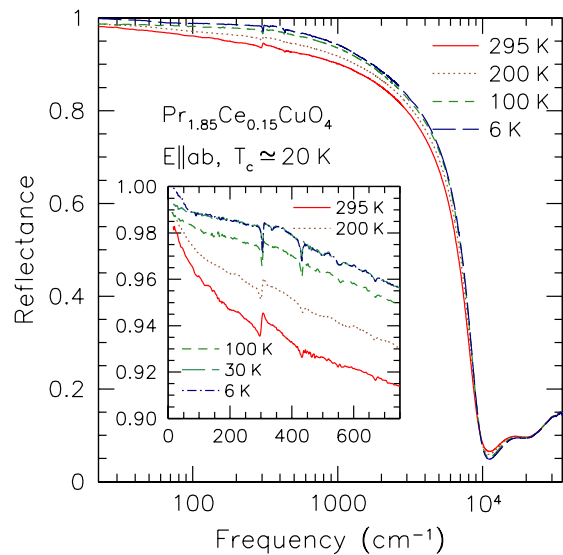


FIG. 1: (Color online) The temperature dependence of the reflectance at a near-normal angle of incidence of single crystal $\text{Pr}_{1.85}\text{Ce}_{0.15}\text{CuO}_4$ ($T_c \simeq 20 \text{ K}$) from ≈ 18 to 34000 cm^{-1} for light polarized in the a - b plane above and below T_c . Inset: The detailed temperature dependence of the far-infrared reflectance above and below T_c . Note the kink and the sudden increase in the reflectance below $\simeq 70 \text{ cm}^{-1}$ for $T \ll T_c$. The sharp features in the reflectance are infrared-active lattice modes. (The resolution is 2 cm^{-1} .)

the reflectance of $\text{Pr}_{1.85}\text{Ce}_{0.15}\text{CuO}_4$ has been employed to about 35 eV ;²⁹ above that frequency a free-electron approximation has been assumed ($R \propto 1/\omega^4$).

III. RESULTS AND DISCUSSION

A. Optical and transport properties

The ab -plane reflectance of $\text{Pr}_{1.85}\text{Ce}_{0.15}\text{CuO}_4$ ($T_c \simeq 20 \text{ K}$) is shown in Fig. 1 over a wide spectral range, at a variety of temperatures above and below T_c . The reflectance in the mid-infrared region and above is consistent with previous studies of electron-doped cuprates;^{24,26,27,28,29,30,31,32,33,34} there is a plasma edge at $\approx 1.2 \text{ eV}$, and the reflectance throughout the mid-infrared region increases with decreasing temperature. The inset in Fig. 1 shows the low-frequency reflectance at several temperatures above and below T_c . The sharp structures in the reflectance that appear variously as resonant and antiresonant features are infrared-active lattice modes.⁴³ The reflectance increases with decreasing temperature, but there is little change between the 30 and 6 K spectra, with the exception of a kink at $\simeq 70 \text{ cm}^{-1}$, below which the reflectance increases rapidly with decreasing frequency. This is the same feature in the reflectance that was observed in thin-film studies,³⁶ that signals the formation of a superconducting energy gap.

The optical conductivity is shown over a wide fre-

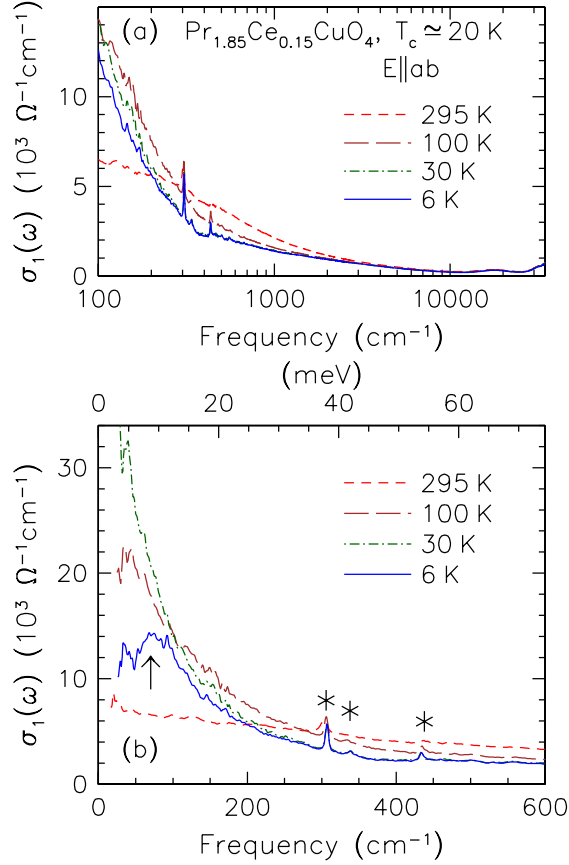


FIG. 2: (Color online) (a) The temperature dependence of the real part of the optical conductivity over a wide frequency range for $\text{Pr}_{1.85}\text{Ce}_{0.15}\text{CuO}_4$ above and below T_c for light polarized in the a - b planes. (b) The low-frequency optical conductivity. The conductivity in the normal state is described by a Drude component that narrows rapidly with decreasing temperature. Below T_c , there is a significant loss of spectral weight at low frequency (arrow) due to the formation of a condensate. The sharp features superimposed upon the electronic background at $\simeq 306$, 338 , and 433 cm^{-1} (asterisks) are infrared-active phonon modes.⁴³

quency range in Fig. 2(a), and at low frequency in Fig. 2(b). The conductivity in the normal-state can be described as a combination of a coherent Drude component that describes the far infrared response, and an incoherent component that dominates the mid infrared region. The “two-component” expression for the real part of the optical conductivity is

$$\sigma_1(\omega) = \frac{1}{4\pi} \frac{\omega_{pd}^2 \Gamma}{\omega^2 + \Gamma^2} + \sigma_{\text{MIR}}, \quad (1)$$

where $\omega_{pd}^2 = 4\pi n_d e^2 / m^*$ is the square of the Drude plasma frequency, n_d is a carrier concentration associated with coherent transport, m^* is an effective mass, $\Gamma = 1/\tau$ is the scattering rate, and σ_{MIR} is the mid-infrared component. [When ω_{pd} and $1/\tau$ are in cm^{-1} , σ_1 also has the units cm^{-1} ; to recover units for the conductivity of $\Omega^{-1}\text{cm}^{-1}$, the term $1/4\pi$ in Eq. (1) should

be replaced with $2\pi/Z_0$, where $Z_0 = 377 \Omega$ is the characteristic impedance of free space.] The Drude contribution has the form of a Lorentz oscillator centered at zero frequency. The features in the reflectance attributed to lattice modes appear as sharp resonances in the conductivity, shown in detail in Fig. 2(b). To apply the two-component model to the data, it is necessary to specify the nature of σ_{MIR} . The mid-infrared conductivity is often described by a series of overdamped Lorentzian oscillators which yield a flat, incoherent response in this region. However, this approach can be somewhat arbitrary. To simplify the fitting a constant background ($\sigma_{\text{MIR}} \simeq 1000 \Omega^{-1}\text{cm}^{-1}$) has been used at low temperature. The fitted results show that while the scattering rate decreases from $1/\tau = 130 \pm 3$ to $80 \pm 2 \text{ cm}^{-1}$ when the temperature is reduced from 100 K to just above T_c at 30 K, the Drude plasma frequency remains constant at $\omega_{pd} = 13000 \pm 200 \text{ cm}^{-1}$. Transport measurements in the electron-doped cuprates typically show a quadratic form of the resistivity,^{17,44,45,46,47} $\rho = \rho_0 + aT^2$, with a weak temperature dependence near T_c , indicating that at low temperatures $1/\tau$ is dominated by ρ_0 . Interestingly, the result that $\hbar/\tau \approx 2k_B T$ close to T_c seems to be true for many of the cuprates.

Note that ω_{pd}^2 is a reflection of only those carriers that participate in coherent transport, rather than the total number of doped carriers determined from the classical plasma frequency $\omega_p^2 = 4\pi n e^2 / m$. The value for ω_p may be estimated using several different techniques. The zero-crossing of the real part of the dielectric function $\epsilon_1(\omega)$ occurs at $\omega_p / \sqrt{\epsilon_\infty}$. However, the presence of interband absorptions that overlap with the coherent component, as well as the difficulty in choosing the correct value of ϵ_∞ , makes this approach unreliable. Another method is the finite-energy f -sum rule⁴⁸

$$\int_0^{\omega_c} \sigma_1(\omega) d\omega \approx \omega_p^2 / 8, \quad (2)$$

where ω_c is a cut-off frequency. In the absence of other excitations, this sum rule is exact in the $\omega_c \rightarrow \infty$ limit. While this condition is difficult to achieve in the cuprates, modifications to this sum rule based on an analysis of the absorption coefficient $\alpha(\omega)$ have been suggested by Hwang *et al.*⁴⁹ Adopting this approach yields $\omega_p \simeq 19300 \text{ cm}^{-1}$, suggesting that only about half of the doped carriers participate in coherent transport (assuming the masses do not change), similar to the hole-doped materials.⁵⁰

While the majority of this paper is concerned with the far-infrared optical properties, it is worth commenting briefly on the behavior of the optical conductivity throughout the rest of the infrared frequency range. As Fig. 2(a) indicates, at room temperature the conductivity is quite broad, with little frequency dependence at low energies; however, as the temperature decreases the Drude component narrows rapidly. The reduction in $1/\tau$ leads to changes in the conductivity over much of the far infrared; however, with the exception of a weak feature at

$\simeq 18\,000\text{ cm}^{-1}$, the high-frequency conductivity displays little structure. While this result is consistent with an earlier study of single crystal $\text{Nd}_{1.85}\text{Ce}_{0.15}\text{CuO}_4$ grown by a flux technique,³⁰ other works on crystals grown using the traveling-solvent floating-zone method have revealed some unusual structure in the $300 - 400\text{ cm}^{-1}$ ($40 - 50\text{ meV}$) region.^{24,32,33} The as-grown electron-doped materials are not superconducting; they must be oxygen-reduced to induce a T_c . Interestingly, the as-grown (or oxygenated) samples show prominent structure in the reflectance in the $300 - 400\text{ cm}^{-1}$ region that manifests itself as a suppression of the conductivity, that is almost completely removed upon oxygen reduction.^{31,32} We speculate that the differences observed in the various works may be related to different levels of oxygen reduction. As previously mentioned, the conductivity is reasonably well described in the far-infrared region by a Drude response. However, it has been noted in the hole-doped cuprates that the modulus of the conductivity obeys a power law over much of the mid-infrared region,^{51,52} $|\tilde{\sigma}(\omega)| \propto \omega^{-0.65}$. The log-log plot of the temperature dependence of the modulus of the optical conductivity vs frequency is shown in Fig. 3 for a variety of temperatures over a wide frequency range. Throughout much of the mid infrared, the modulus of the conductivity follows the power law $|\tilde{\sigma}(\omega)| \propto \omega^{-0.69}$, in good agreement with the behavior observed in the hole-doped cuprates.^{51,52,53,54,55,56} Below roughly 1000 cm^{-1} there is a deviation from this power-law behavior at high temperature. As the temperature decreases a linear behavior is once again recovered; however, the exponent is now larger $|\tilde{\sigma}(\omega)| \propto \omega^{-0.81}$, suggesting that the character of the conductivity is different in these two regions.

Well below T_c , there is a substantial reduction in the low-frequency conductivity [indicated by the arrow in Fig. 2(b)]. The Ferrell-Glover-Tinkham (FGT) sum rule^{57,58} states that the difference between the conductivity curves at $T \simeq T_c$ and $T \ll T_c$ (the so-called “missing area”) is related to the formation of a superconducting condensate

$$\int_0^{\omega_c} [\sigma_1(\omega, T \simeq T_c) - \sigma_1(\omega, T \ll T_c)] \approx \omega_{ps}^2/8, \quad (3)$$

where $\omega_{ps}^2 = 4\pi n_s e^2/m^*$ is the square of the superconducting plasma frequency, n_s is the superconducting carrier concentration, and ω_c is chosen such that ω_{ps}^2 converges smoothly. The strength of the condensate is simply $\rho_s = \omega_{ps}^2$, which is related to the penetration depth by $\rho_s = c^2/\lambda^2$. The value of ρ_s may also be estimated from the response of the dielectric function in the zero-frequency limit to the formation of a condensate, which is expressed purely by the real part $\epsilon_1(\omega \rightarrow 0) = \epsilon_\infty - \omega_{ps}^2/\omega^2$ for $T \ll T_c$. This allows the strength of the condensate to be calculated from $\omega_{ps}^2 \simeq -\omega^2 \epsilon_1(\omega)$ as $\omega \rightarrow 0$. The frequency dependence of $\sqrt{-\omega^2 \epsilon_1(\omega)}$ is shown in Fig. 4 for $\text{Pr}_{1.85}\text{Ce}_{0.15}\text{CuO}_4$ at 30 and 6 K. The low-frequency extrapolations employed

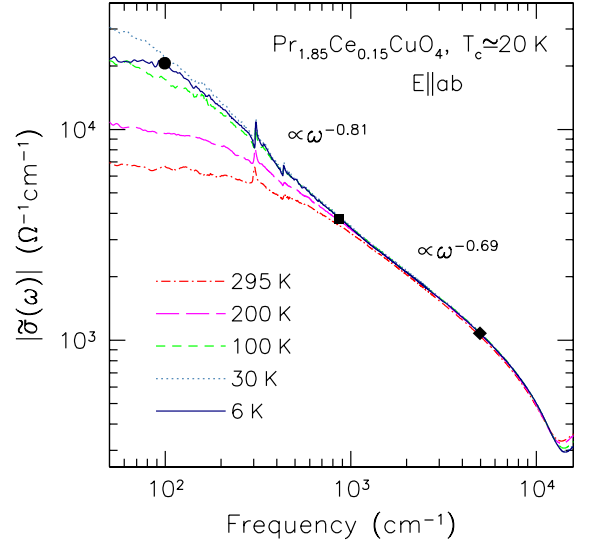


FIG. 3: (Color online) The log-log plot of the temperature dependence of the modulus of the optical conductivity over a wide frequency range above and below T_c . Throughout the mid-infrared region (between the square and the diamond), the modulus obeys a power-law behavior, $|\tilde{\sigma}(\omega)| \propto \omega^{-0.7}$. At low temperature the power-law behavior is recovered again at low frequency (between the square and the dot), $|\tilde{\sigma}(\omega)| \propto \omega^{-0.8}$. From the relation $\tilde{\sigma}(\omega) = \sigma_1(\omega) + i\sigma_2(\omega) = -i\omega[\tilde{\epsilon}(\omega) - \epsilon_\infty]/4\pi$, a value of $\epsilon_\infty = 3.6$ was used to determine $\sigma_2(\omega)$.]

in the Kramers-Kronig analysis of the reflectance are included to allow the $\omega \rightarrow 0$ values to be determined more easily. In the normal state the function goes smoothly to zero, indicating the absence of a condensate. Well below T_c , the estimate for the superconducting plasma frequency is $\omega_{ps} \simeq 7800\text{ cm}^{-1}$. This is consistent with values of $\omega_{ps} \simeq 8000\text{ cm}^{-1}$ determined from the FGT sum rule. From $1/\lambda = 2\pi\omega_{ps}$ the penetration depth is determined to be $\lambda = 2000 \pm 100\text{ Å}$, similar to results obtained from thin films with similar T_c 's.^{36,59} A comparison of ω_{ps} to ω_{pd} indicates that less than half of the carriers involved in the coherent Drude component have collapsed into the condensate (assuming similar effective masses), a result that is consistent with the larger body of work on the hole-doped materials.⁵⁰

The relatively low values for T_c and λ for this material, and the electron-doped materials in general, have always presented a challenge for the Uemura plot,⁶⁰ which relates the density of carriers in the superfluid to the transition temperature, $\rho_s \propto T_c$. While the Uemura plot works well for the hole-doped cuprates in the underdoped region, the electron-doped materials have typically fallen well off of the Uemura plot.^{30,61,62} Recently, a more general scaling relation $\rho_s \propto \sigma_{dc} T_c$ (where σ_{dc} is determined just above T_c) which allows the points for the electron- and hole-doped cuprates to be scaled onto the same universal line.^{38,39} The value of σ_{dc} close to T_c is taken from both $\sigma_1(\omega \rightarrow 0)$ as well as Drude fits to the lineshape of the conductivity, resulting in the estimate $\sigma_{dc}(T \approx T_c) = 35\,000 \pm 3000\text{ Ω}^{-1}\text{cm}^{-1}$; this places

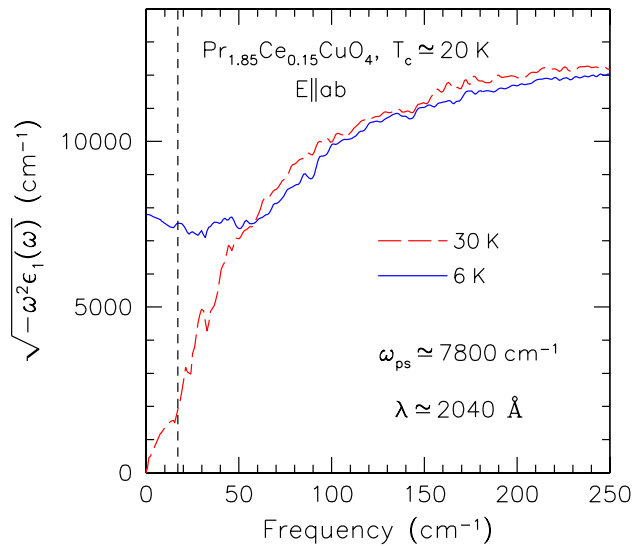


FIG. 4: (Color online) The temperature dependence of $\sqrt{-\omega^2 \epsilon_1(\omega)}$ of $\text{Pr}_{1.85}\text{Ce}_{0.15}\text{CuO}_4$ at 30 and 6 K. The results of the low-frequency extrapolations employed in the Kramers-Kronig analysis below $\approx 18 \text{ cm}^{-1}$ (dashed line) are included as a guide to the eye.

the material almost directly on the $\rho_s \propto \sigma_{dc} T_c$ scaling line. An implication of this result is the suggestion that this material is not in the clean limit;³⁹ this controversial point will be examined in more detail in a subsequent section.

B. Determination of the gap maximum

A reasonable estimate for the gap maximum may be taken from a comparison of the reflectance at $T \approx T_c$ and $T \ll T_c$, shown in Fig. 5(a). Above about 70 cm^{-1} the two curves are nearly identical, but below this value the 6 K reflectance displays a kink followed by an abrupt increase; this feature has also been observed in our measurements of the reflectance of thin films of this material.³⁶ The optical conductivity (and by extension, the reflectance) of a material may be described by the Kubo-Greenwood formula, which considers all the single-electron transitions across the Fermi surface, a measure of the JDOS.⁶³ It is not possible to reproduce the structure in the reflectance simply by considering the response of the dielectric function to the formation of a condensate; instead, the kink is associated with a DOS effect due to the formation of a superconducting gap. From the JDOS, the position of the kink should correspond to twice the gap maximum. A reasonable estimate for twice the gap maximum is therefore $2\Delta_0 \approx 70 \text{ cm}^{-1}$, or $\Delta_0 \approx 4.3 \text{ meV}$; this yields a ratio of $2\Delta_0/k_B T_c \approx 5$, in good agreement with previous thin film³⁶ and single crystal results.⁶⁴ Furthermore, the value for Δ_0 is in excellent agreement with the values determined from Raman studies.^{18,19}

The nature of the superconducting energy gap also

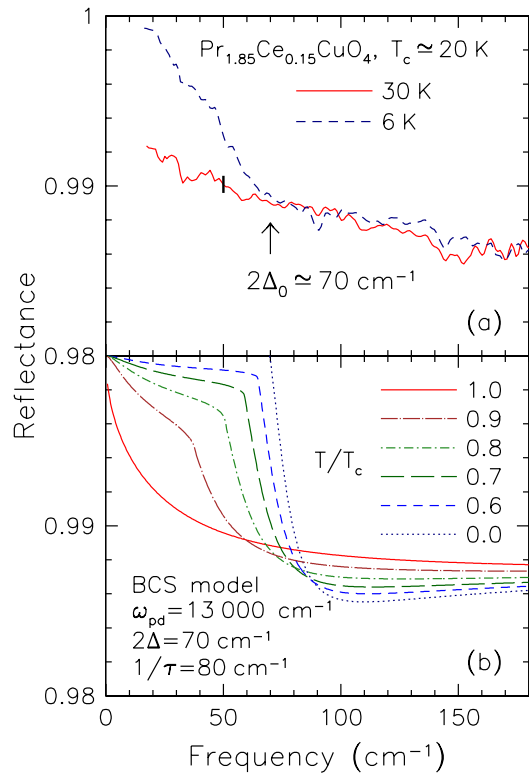


FIG. 5: (Color online) (a) The far-infrared reflectance of $\text{Pr}_{1.85}\text{Ce}_{0.15}\text{CuO}_4$ above and below T_c . The kink in the reflectance below T_c signals the formation of a superconducting energy gap and denotes the value of $2\Delta_0$. The estimated noise in the reflectance is indicated by the thick line at 50 cm^{-1} ; the S/N is in excess of 2000 : 1, and no smoothing has been applied to the data. (b) The calculated reflectance of a BCS superconductor with an isotropic s -wave gap for a series of temperatures at and below T_c .

plays a critical role in our ability to observe it. Gaps with sharp features in the DOS, and therefore the JDOS, should have features that are more easily observed in the optical properties. To illustrate this point, gap functions for isotropic s -wave, monotonic and nonmonotonic d -wave materials are shown in Fig. 6(a) and $\Delta(\phi)/\Delta_0$ is shown over the first quadrant in Fig. 6(b). The non-monotonic d -wave gap will have a gap maximum much closer to the nodes, resulting in a larger part of the Fermi surface that is effectively gapped. In comparison, the monotonic d -wave gap associated with the hole-doped cuprates has a gap maximum far from the nodal regions and the resulting JDOS is rather smeared out. We propose that the non-monotonic nature of the d -wave gap in the electron-doped material makes it possible to identify Δ_0 from the optical properties. However, this is by no means restricted to the electron-doped materials. There are large changes observed in the reflectance of the hole-doped cuprates below T_c , the so-called “knee” in the reflectance⁶⁵ located at roughly $2\Delta_0$, that may be due to DOS effects related to the formation of a superconducting energy gap.⁶⁶ In those cases where this feature

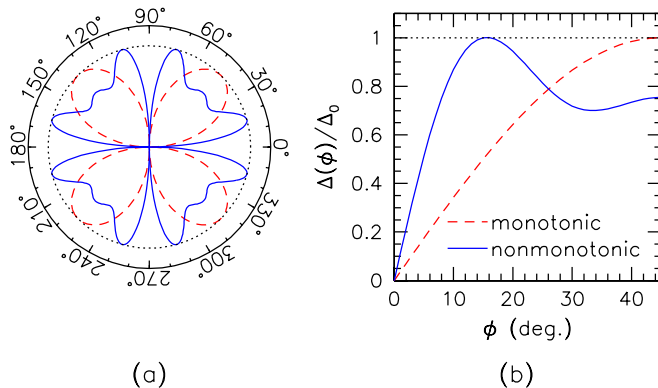


FIG. 6: (Color online) (a) A radial plot of the amplitude of an isotropic s -wave gap (dotted line), a monotonic d -wave gap, $\Delta(\phi) = \Delta_0 \cos(2\phi)$ (dashed line), and a nonmonotonic d -wave gap, $\Delta(\phi) = \Delta_0 [\cos(2\phi) - 0.42 \cos(6\phi) + 0.17 \cos(10\phi)]$. Note that the gap functions are rotated by 45° with respect to the hole-doped cuprates. (b) A linear plot of the same gap functions over the first quadrant.

was observed above T_c , it was argued that it was not related to the superconductivity. However, many of the cuprate superconductors initially studied were naturally underdoped; these materials display a pseudogap that develops in the normal state.⁷ Angle resolved photoemission spectroscopy has demonstrated that the pseudogap entails a partial gapping of the Fermi surface in a manner similar to that of the superconducting energy gap.⁶⁷ In addition, the calculations of the optical conductivity based on a monotonic d -wave gap are in excellent agreement with the experiment.⁶⁸ Thus, the appearance of the knee in the reflectance above T_c in the underdoped materials does not rule out the association of this feature with the superconducting energy gap for $T \ll T_c$.

While it is therefore possible to observe the DOS effects of the superconducting gap in materials with a simple monotonic d -wave gap, we argue that this task is simplified considerably if the gap is nonmonotonic. To elaborate on this point, we calculate the temperature dependence of the reflectance of a material using the BCS model with an isotropic s -wave gap for an arbitrary purity level.⁶⁹ The normal-state is described using the Drude model with a plasma frequency of $\omega_{pd} = 13000 \text{ cm}^{-1}$ and scattering rate $1/\tau = 80 \text{ cm}^{-1}$, while below T_c the optical properties have been calculated with a gap of $2\Delta = 70 \text{ cm}^{-1}$. The calculated reflectance curves are shown in Fig. 5(b). The normal-state reflectance at T_c is reproduced quite well, while below T_c the formation of an isotropic s -wave gap produces a region of steadily increasing reflectance for $\omega \lesssim 2\Delta_0$; for $T \ll T_c$ the gap is fully formed and the reflectance is unity below $2\Delta_0$. While it is clear that the gap in $\text{Pr}_{1.85}\text{Ce}_{0.15}\text{CuO}_4$ is d wave, the nonmonotonic nature of the gap results in more of the Fermi surface being more effectively gapped than the monotonic case (reminiscent of an isotropic gap), resulting in a JDOS which allows for the unambiguous de-

TABLE I: The estimated values at the nodal and antinodal points of the Fermi surface for the Fermi velocity, scattering rate and mean-free path ($T \gtrsim T_c$); the magnitude of the superconducting energy gap and the coherence length ($T \ll T_c$).

Region	v_F^a (10^7 cm/s)	$1/\tau$ (cm^{-1})	l (\AA)	$\Delta(\phi)$ (meV)	$\xi_{0,calc}^b$ (\AA)
nodal	2.5	< 80	> 1000	$\rightarrow 0$	$\rightarrow \infty$
antinodal	0.5	80	250	4.3	165

^aThe experimental error is $\sim 20 - 30\%$.

^bThe coherence length is calculated from $\xi_0 = v_F/(\sqrt{12}\Delta)$.

termination of $2\Delta_0$.

C. Anisotropy and the effects of disorder

In terms of the optically-determined values for $1/\tau$ and $2\Delta_0$, the clean and dirty limits are defined as $1/\tau \ll 2\Delta_0$ and $1/\tau \gtrsim 2\Delta_0$, respectively (where it is understood that “dirty” refers to the effects of disorder and electronic correlations rather than impurity effects). Although the cuprates are generally considered to be in the clean limit, we now are faced with the condition that $1/\tau \approx 2\Delta_0$, which places the material close to the dirty limit. The widely-accepted statement that this class of materials is in the clean limit is based on the incorrect comparison of the small value for the quasiparticle scattering along the nodal direction and the gap value along the antinodal direction, two different directions in momentum space. This statement does not take into consideration the anisotropic nature of the Fermi surface of these materials in which both $1/\tau$ and the superconducting energy gap vary significantly, depending on whether the nodal or antinodal directions are being considered. For instance, the quasiparticle scattering rate is observed to drop abruptly in the cuprates below T_c after the antinodal region of the Fermi surface is gapped, suggesting that the scattering rate in the nodal direction is much smaller than the antinodal direction.^{70,71} (In the underdoped cuprates the formation of a pseudogap leads to much the same behavior in the normal state; the gapping of the antinodal regions restricts the quasiparticles to the nodal part of the Fermi surface, where they display a metallic character,^{66,72} i.e., a “nodal metal”). In the absence of a pseudogap, Matthiesen’s rule implies that the $1/\tau$ observed in the normal state therefore arises from scattering mainly in the antinodal direction, and that as a consequence $1/\tau$ is anisotropic. In addition, the superconducting energy gap is highly-anisotropic due to its d -wave nature, with Δ_0 in this work estimated to be $\simeq 4.3 \text{ meV}$. The comparison of the normal-state scattering rate with the superconducting energy gap maximum correctly compares two quantities associated with the antinodal direction.

In terms of the mean free path l and the superconducting coherence length ξ_0 , the clean and dirty limits are ex-

pressed as $l \gg \xi_0$ and $l \leq \xi_0$, respectively. Allowing that the mean free path is simply the Fermi velocity times the scattering time, $l = v_F \tau$, and that the coherence length for an isotropic gap in the weak-coupling regime is $\xi_0 \simeq v_F / (\sqrt{12} \Delta)$ (Ref. 73), then the statement that $1/\tau \approx 2\Delta_0$ and $l \approx \xi_0$ are roughly equivalent. In a previous study of $\text{Nd}_{1.85}\text{Ce}_{0.15}\text{CuO}_4$, it was determined that $1/\tau \approx 100 \text{ cm}^{-1}$ just above T_c (Ref. 30). Using an average value for the Fermi velocity of $v_F = 2.2 \times 10^7 \text{ cm/s}$ (Ref. 74) yields $l \approx 730 \text{ \AA}$. Given that $\xi_0 \simeq 80 - 90 \text{ \AA}$ in the electron-doped materials,^{75,76} this appeared to justify the statement that this material was in the clean limit, contradicting the present result. However, in addition to $1/\tau$, the anisotropy of the Fermi velocity is also well documented in the high-temperature superconductors, and is found to vary from $v_F \approx 2.5 - 2.7 \times 10^7 \text{ cm/s}$ along the nodal direction,^{77,78} to $v_F \approx 0.5 \times 10^7 \text{ cm/s}$ along the antinodal direction;⁷⁹ while these values appear to be remarkably universal, some sample and doping dependence is expected. Thus, the mean free path determined from $1/\tau$ should be based on the antinodal v_F ; this yields a significantly smaller value of $l \simeq 250 \text{ \AA}$. Based on the anisotropy of the Fermi velocity alone, the mean free path along the nodal direction will be considerably larger. The estimated value Δ_0 in the present work is $\simeq 4.3 \text{ meV}$; using the value for the antinodal Fermi velocity yields $\xi_{0,calc} \simeq 165 \text{ \AA}$, which is about twice as large as the commonly quoted experimental values of $\xi_0 = 80 - 90 \text{ \AA}$; the lack of perfect agreement may be partially due to the uncertainty in v_F , but it is more likely a result of the naïve approach taken to calculate ξ_0 . In the nodal direction, the gap vanishes and the coherence length diverges. These results are summarized in Table I.

What these calculations indicate is that the assertion that $l \gg \xi_0$ arises only if the mean free path along the nodal direction is compared with the coherence length in the antinodal direction; if the nodal and antinodal directions are considered as separate cases, then it is indeed the case that $l \approx \xi_0$. Thus, the result that $1/\tau \approx 2\Delta_0$ is in fact consistent with the statement that $l \approx \xi_0$, where it is understood that we are referring to the antinodal di-

rection. In fact, the statement $1/\tau \approx 2\Delta_0$ should be considered more robust because it does not rely on v_F . This implies that the material is not in the clean limit. Note that this statement should be qualitatively correct along the nodal direction as well, but because precise values of l and ξ_0 [or $1/\tau$ and $\Delta(\phi)$] are difficult to determine, this statement is somewhat speculative.

IV. CONCLUSIONS

The *ab*-plane optical properties of single crystal $\text{Pr}_{1.85}\text{Ce}_{0.15}\text{CuO}_4$ ($T_c \simeq 20 \text{ K}$) have been examined above and below T_c . In the normal state just above T_c , the coherent part of the optical conductivity may be described by a simple Drude component with $\omega_{pd} \simeq 13000 \text{ cm}^{-1}$ and $1/\tau \simeq 80 \text{ cm}^{-1}$. It is noted that the condition $\hbar/\tau \approx 2k_B T$ near T_c observed in this material is generally true for many other cuprate superconductors. Below T_c , the superconducting plasma frequency is estimated to be $\omega_{ps} \simeq 7800 \text{ cm}^{-1}$, yielding a penetration depth of $\lambda \simeq 2000 \text{ \AA}$; when combined with the optical estimate for the dc resistivity σ_{dc} just above T_c , this material falls on the scaling relation $\rho_s \propto \sigma_{dc} T_c$ recently proposed for the cuprate superconductors.^{38,39} The estimate for the superconducting gap maximum $2\Delta_0 \simeq 70 \text{ cm}^{-1}$ is in good agreement with previous results,^{18,36} and is consistent with the view that the superconducting energy gap is most likely nonmonotonic *d* wave. The result that $1/\tau \approx 2\Delta_0$ implies that this material is not in the clean limit, a self-consistent result that by its own nature allows for the direct observation of the superconducting energy gap.

We would like to acknowledge helpful discussions with D. N. Basov, A. V. Chubukov, A. J. Millis, T. Valla and N. L. Wang. This work was supported by the Office of Science, U.S. Dept. of Energy, under contract number DE-AC02-98CH10886; work in Maryland is supported by the NSF contract DMR-0352735.

* Electronic address: homes@bnl.gov

¹ Y. Tokura and S. Uchida, *Nature (London)* **377**, 345 (1989).

² H. Takagi, S. Uchida, and Y. Tokura, *Phys. Rev. Lett.* **62**, 1197 (1989).

³ T. Siegrist, S. M. Zahurak, D. W. Murphy, and R. S. Roth, *Nature (London)* **334**, 231 (1988).

⁴ M. G. Smith, A. Manthiram, J. Zhou, J. B. Goodenough, and J. T. Markert, *Nature (London)* **351**, 549 (1991).

⁵ A. Damascelli, Z. Hussain, and Z.-X. Shen, *Rev. Mod. Phys.* **75**, 473 (2003).

⁶ G. M. Luke, L. P. Le, B. J. Sternlieb, Y. J. Uemura, J. H. Brewer, R. Kadano, R. F. Kiefl, S. R. Kreitzman, T. M. Riseman, C. E. Stroinach, et al., *Phys. Rev. B* **42**, 7981 (1990).

⁷ T. Timusk and B. Statt, *Rep. Prog. Phys.* **62**, 61 (1999).

⁸ P. K. Mang, O. P. Vajk, A. Arvanitaki, J. W. Lynn, and M. Greven, *Phys. Rev. Lett.* **93**, 027002 (2004).

⁹ Q. Huang, J. F. Zasadzinski, N. Tralshawala, K. E. Gray, D. G. Hinks, J. L. Peng, and R. L. Greene, *Nature (London)* **347**, 369 (1990).

¹⁰ B. Stadlober, G. Krib, R. Nemetschek, R. Hackl, J. L. Cobb, and J. T. Markert, *Phys. Rev. Lett.* **74**, 4911 (1995).

¹¹ C. C. Tsuei and J. R. Kirtley, *Phys. Rev. Lett.* **85**, 182 (2000).

¹² A. Biswas, P. Fournier, V. N. Smolyaninova, R. C. Budhani, J. S. Higgins, and R. L. Greene, *Phys. Rev. B* **64**, 104519 (2001).

¹³ N. P. Armitage, D. H. Lu, D. L. Feng, C. Kim, A. Damascelli, K. M. Shen, F. Ronning, and Z.-X. Shen, *Phys. Rev.*

- Lett. **86**, 1126 (2001).
- ¹⁴ T. Sato, T. Kamiyama, T. Takahashi, K. Kurahashi, and K. Yamada, *Science* **291**, 1517 (2001).
 - ¹⁵ J. D. Kokales, P. Fournier, L. V. Mercaldo, V. V. Talanov, R. L. Greene, and S. M. Anlage, *Phys. Rev. Lett.* **85**, 3696 (2000).
 - ¹⁶ R. Prozorov, R. W. Giannetta, P. Fournier, and R. L. Greene, *Phys. Rev. Lett.* **85**, 3700 (2000).
 - ¹⁷ J. A. Skinta, M.-S. Kim, T. R. Lemberger, T. Greibe, and M. Naito, *Phys. Rev. Lett.* **88**, 207005 (2002).
 - ¹⁸ G. Blumberg, A. Koitzsch, A. Gozar, B. S. Dennis, C. A. Kendziora, P. Fournier, and R. L. Greene, *Phys. Rev. Lett.* **88**, 107002 (2002).
 - ¹⁹ G. Blumberg, A. Koitzsch, A. Gozar, B. S. Dennis, C. A. Kendziora, P. Fournier, and R. L. Greene, *Phys. Rev. Lett.* **90**, 149702 (2003).
 - ²⁰ H. Matsui, K. Terashima, T. Sato, T. Takahashi, and K. Yamada, *Phys. Rev. Lett.* **95**, 017003 (2005).
 - ²¹ L. Shan, Y. Huang, H. Gao, Y. Wang, S. L. Li, P. D. Dai, F. Zhou, J. W. Xiong, W. X. Ti, and H. H. Wen, *Phys. Rev. B* **72**, 144506 (2005).
 - ²² D. V. Harlingen, *Rev. Mod. Phys.* **67**, 515 (1995).
 - ²³ C. C. Tsuei and J. R. Kirtley, *Rev. Mod. Phys.* **72**, 969 (2000).
 - ²⁴ Y. Onose, Y. T. an K. Ishizaka, and Y. Tokura, *Phys. Rev. Lett.* **87**, 217001 (2001).
 - ²⁵ A. Zimmers, J. M. Tomczak, R. P. S. M. Lobo, N. Bontemps, C. P. Hill, M. C. Barr, Y. Dagan, R. L. Greene, A. J. Millis, and C. C. Homes, *Europhys. Lett.* **70**, 225 (2005).
 - ²⁶ S. L. Cooper, G. A. Thomas, J. Orenstein, D. H. Rapkine, A. J. Millis, S.-W. Cheong, A. S. Cooper, and Z. Fisk, *Phys. Rev. B* **41**, 11605 (1990).
 - ²⁷ J.-G. Zhang, X.-X. Bi, E. McRae, P. C. Ecklund, B. C. Sales, and M. Mostoller, *Phys. Rev. B* **43**, 5389 (1991).
 - ²⁸ S. Lupi, P. Calvani, M. Capizzi, P. Maselli, W. Sadowski, and E. Walker, *Phys. Rev. B* **45**, 12470 (1992).
 - ²⁹ T. Arima, Y. Tokura, and S. Uchida, *Phys. Rev. B* **48**, 6597 (1993).
 - ³⁰ C. C. Homes, B. P. Clayman, J. L. Peng, and R. L. Greene, *Phys. Rev. B* **56**, 5525 (1997).
 - ³¹ Y. Onose, Y. Taguchi, T. Ishikawa, S. Shinomori, K. Ishizaka, and Y. Tokura, *Phys. Rev. Lett.* **82**, 5120 (1999).
 - ³² E. J. Singley, D. N. Basov, K. Kurahashi, T. Uefuji, and K. Yamada, *Phys. Rev. B* **64**, 224503 (2001).
 - ³³ Y. Onose, Y. Taguchi, K. Ishizaka, and Y. Tokura, **69**, 024504 (2004).
 - ³⁴ N. L. Wang, G. Li, D. Wu, X. H. Chen, C. H. Wang, and H. Ding, *Phys. Rev. B* **73**, 184502 (2006).
 - ³⁵ K. Kamarás, S. L. Herr, C. D. Porter, N. Tache, D. B. Tanner, S. Etemad, T. Venkatesan, E. Chase, A. Inam, X. D. Wu, et al., *Phys. Rev. Lett.* **64**, 84 (1990), see also the erratum in **64**, 1692 (1990).
 - ³⁶ A. Zimmers, R. P. S. M. Lobo, N. Bontemps, C. C. Homes, M. C. Barr, Y. Dagan, and R. L. Greene, *Phys. Rev. B* **70**, 132502 (2004).
 - ³⁷ A. J. Millis, A. Zimmers, R. P. S. M. Lobo, N. Bontemps, and C. C. Homes, *Phys. Rev. B* **72**, 224517 (2005).
 - ³⁸ C. C. Homes, S. V. Dordevic, M. Strongin, D. A. Bonn, R. Liang, W. N. Hardy, S. Komiya, Y. Ando, G. Yu, N. Kaneko, et al., *Nature (London)* **430**, 539 (2004).
 - ³⁹ C. C. Homes, S. V. Dordevic, T. Valla, and M. Strongin, *Phys. Rev. B* **72**, 134517 (2005).
 - ⁴⁰ J. L. Peng, Z. Y. Li, and R. L. Greene, *Physica C* **177**, 79 (1991).
 - ⁴¹ M. Brinkmann, T. Rex, H. Bach, and K. Westerholt, *J. of Crystal Growth* **163**, 369 (1996).
 - ⁴² C. C. Homes, M. Reedyk, D. A. Crandles, and T. Timusk, *Appl. Opt.* **32**, 2972 (1993).
 - ⁴³ M. Braden, L. Pintschovius, T. Uefuji, and K. Yamada, *Phys. Rev. B* **72**, 184517 (2005).
 - ⁴⁴ W. Jiang, S. N. Mao, X. X. Xi, X. Jiang, J. L. Peng, T. Venkatesan, C. J. Lobb, and R. L. Greene, *Phys. Rev. Lett.* **73**, 1291 (1994).
 - ⁴⁵ J. L. Peng, E. Maiser, T. Venkatesan, R. L. Greene, and G. Czjzek, *Phys. Rev. B* **55**, R6145 (1997).
 - ⁴⁶ P. Fournier, X. Jiang, W. Jiang, S. N. Mao, T. Venkatesan, C. J. Lobb, and R. L. Greene, *Phys. Rev. B* **56**, 14149 (1997).
 - ⁴⁷ Y. Dagan, M. M. Qazilbash, C. P. Hill, V. N. Kulkarni, and R. L. Greene, *Phys. Rev. Lett.* **92**, 167001 (2004).
 - ⁴⁸ D. Y. Smith, in *Handbook of Optical Constants of Solids*, edited by E. D. Palik (Academic, New York, 1985), pp. 35–68.
 - ⁴⁹ J. Hwang, T. Timusk, A. V. Puchkov, N. L. Wang, G. D. Gu, C. C. Homes, J. J. Tu, and H. Eisaki, *Phys. Rev. B* **69**, 094520 (2004).
 - ⁵⁰ D. B. Tanner, H. L. Liu, , M. A. Quijada, A. M. Zibold, H. Berger, R. J. Kelley, M. Onellion, F. C. Chou, D. C. Johnston, et al., *Physica B* **244**, 1 (1998).
 - ⁵¹ A. E. Azrak, R. Nahoum, N. Bontemps, M. Guilloux-Viry, C. Thivet, A. Perrin, S. Labdi, Z. Z. Li, and H. Raffy, *Phys. Rev. B* **49**, 9846 (1994).
 - ⁵² D. van der Marel, H. J. A. Molegraaf, J. Zaanen, Z. Nussinov, F. Carbone, A. Damascelli, H. Eisaki, M. Greven, P. H. Kes, and M. Li, *Nature* **425**, 271 (2003).
 - ⁵³ P. W. Anderson, *Phys. Rev. B* **55**, 11785 (1997).
 - ⁵⁴ M. R. Norman and A. V. Chubukov, *Phys. Rev. B* **73**, 140501 (2006).
 - ⁵⁵ P. Krotkov and A. V. Chubukov, *Phys. Rev. Lett.* **96**, 107002 (2006).
 - ⁵⁶ P. Krotkov and A. V. Chubukov, cond-mat/0604675.
 - ⁵⁷ R. A. Ferrell and R. E. Glover, III, *Phys. Rev.* **109**, 1398 (1958).
 - ⁵⁸ M. Tinkham and R. A. Ferrell, *Phys. Rev. Lett.* **2**, 331 (1959).
 - ⁵⁹ R. Prozorov, R. W. Giannetta, A. Carrington, P. Fournier, R. L. Greene, P. Guptasarma, D. G. Hinks, and A. R. Banks, *Appl. Phys. Lett.* **77**, 4202 (2000).
 - ⁶⁰ Y. J. Uemura, V. J. Emery, A. R. Moodenbaugh, M. Suenaga, D. C. Johnston, A. J. Jacobson, J. T. Lewandowski, J. H. Brewer, R. F. Kiefl, S. R. Kreitzman, et al., *Phys. Rev. B* **38**, 909 (1998).
 - ⁶¹ A. Shengelaya, R. Khasanov, D. G. Eshchenko, D. D. Castro, I. M. Savić, M. S. Park, K. H. Kim, S.-I. Lee, K. A. Müller, and H. Keller, *Phys. Rev. Lett.* **94**, 127001 (2005).
 - ⁶² C. C. Homes, *Physica C* **445-448**, 8 (2006).
 - ⁶³ W. A. Harrison, *Solid State Theory* (McGraw-Hill, New York, 1970).
 - ⁶⁴ M. M. Qazilbash, A. Koitzsch, B. S. Dennis, A. Gozar, H. Balci, C. A. Kendziora, R. L. Greene, and G. Blumberg, *Phys. Rev. B* **72**, 214510 (2005).
 - ⁶⁵ D. B. Tanner and T. Timusk, in *Physical Properties of High-Temperature Superconductors III*, edited by D. M. Ginsberg (World Scientific, Singapore, 1992), pp. 363–469.
 - ⁶⁶ Y. S. Lee, K. Segawa, Z. Q. Li, W. J. Padilla, M. Dumm, S. V. Dordevic, C. C. Homes, Y. Ando, , and D. N. Basov,

- Phys. Rev. B **72**, 054529 (2005).
- ⁶⁷ A. Kanigel, M. R. Norman, M. Randeria, U. Chatterjee, S. Suoma, A. Kaminski, H. M. Fretwell, S. Rosenkranz, M. Shi, T. Sato, et al., *Nature Physics* **2**, 447 (2006).
 - ⁶⁸ J. P. Carbotte and E. Schachinger, *Phys. Rev. B* **69**, 224501 (2004).
 - ⁶⁹ W. Zimmerman, E. H. Brandt, M. Bauer, E. Seider, and L. Genzel, *Physica C* **183**, 99 (1991).
 - ⁷⁰ D. A. Bonn, R. Liang, T. M. Riseman, D. J. Baar, D. C. Morgan, K. Zhang, P. Dosanjh, T. L. Duty, A. MacFarlane, G. D. Morris, et al., *Phys. Rev. B* **47**, 11314 (1993).
 - ⁷¹ T. Valla, A. V. Fedorov, P. D. Johnson, Q. Li, G. D. Gu, and N. Koshizuka, *Phys. Rev. Lett.* **85**, 828 (2000).
 - ⁷² M. Sutherland, S. Y. Li, D. G. Hawthorn, R. W. Hill, F. Ronning, M. A. Tanatar, J. Paglione, H. Zhang, L. Taillefer, J. DeBenedictis, et al., *Phys. Rev. Lett.* **94**, 147004 (2005).
 - ⁷³ L. Benfatto, A. Toschi, S. Capara, and C. Castellani, *Phys. Rev. B* **66**, 054515 (2002).
 - ⁷⁴ P. B. Allen, W. E. Pickett, and H. Krakauer, *Phys. Rev. B* **37**, 7482 (1988).
 - ⁷⁵ S. M. Anlage, D.-H. Wu, J. Mao, S. N. Mao, X. X. Xi, T. Venkatesan, J. L. Peng, and R. L. Greene, *Phys. Rev. B* **50**, 523 (1994).
 - ⁷⁶ S. D. Wilson, P. Dai, S. Li, S. Chi, H. J. Kang, and J. W. Lynn, *Nature (London)* **442**, 59 (2006).
 - ⁷⁷ J. Mesot, M. R. Norman, H. Ding, M. Randeria, J. C. Campuzano, A. Paramekanti, H. M. Fretwell, A. Kaminski, T. Takeuchi, T. Yokoya, et al., *Phys. Rev. Lett.* **83**, 840 (1999).
 - ⁷⁸ X. J. Zhou, T. Yoshida, A. Lanzara, P. V. Bogdanov, S. A. Kellar, K. M. Shen, W. L. Yang, F. Ronning, T. Sasagawa, T. Kakeshita, et al., *Nature (London)* **423**, 398 (2003).
 - ⁷⁹ A. Damascelli (private communication).